Uncertainty Modelling for Detecting Friction-induced Pad-mode Instabilities in Disc Brake Squeal

S. Oberst*, J.C.S. Lai

Acoustics & Vibration Unit,
School of Engineering and Information Technology,
The University of New South Wales, Australian Defence Force Academy,
Canberra, ACT 2600, Australia

ABSTRACT

Since the early 1930s, brake squeal has been a problem for NVH departments and the high-pitched noise causes customers to complain and lodge costly warranty claims. Due to its friction-induced nature, material properties and operating conditions, the problem of brake squeal is non-linear and highly complex. In the past, research has been focussed on mode-coupling instability predicted by the complex eigenvalue analysis (CEA). However, for unstable modes not detected by CEA, friction-induced energy fed back by the pad modes, due to the friction coefficient, pressure variations and non-linear material properties, has been shown, by means of non-linear time series analyses and the acoustic boundary element method, to cause friction-induced pad squeal or to amplify the mode coupling of brake components for a pad-on-plate system. It is suggested that pad mode instabilities be treated as a stochastic process defined by a random 3-parameter-space: the mean changes in kinetic energy, frequency and acoustic power caused by changes in pressure or the friction coefficient. It is shown that, for a pad-on-plate system and a pad-on-disc simplified brake system, this stochastic approach enables the probability to be calculated for a specified increase in kinetic energy or a specified change in frequencies, thus allowing the assessment of brake squeal propensity and the development of strategies for controlling brake squeal.

INTRODUCTION

In automotive industry brake squeal has become an important cost factor because of customer dissatisfaction. In North America, up to one billion dollars p.a. were spent on Noise, Vibration and Harshness (NVH) issues [1] while friction material suppliers allocated more than half their budgets to dealing with NVH problems [2]. According to a J.D. Power survey conducted in 2002, 60% of warranty claims concerning the brake corner are due to brake squeal [3]. Up to 5% of the USA's gross national product can be accounted for by losses due to friction and wear, which includes brake noise related problems [4].

There have been numerous literature reviews on disc brake squeal recently. Three of the most comprehensive include: Akay [1], in which a general outline of the acoustics of friction concerning not only brake squeal is given; Kinkaid et al. [5] who discuss brake squeal mechanisms; and Ouyang et al. [6] who focus on the numerical analysis of brake squeal noise using the Finite Element Analysis (FEM) in the frequency and time domain. Mechanisms investigated so far which are thought to be responsible for brake squeal include stick-slip [7–9], negative gradient of friction coefficient with sliding velocity $\frac{\partial \mu_k}{\partial v_s}$ [10], sprag-slip [11], mode coupling or binary flutter [12], hammering [13], parametric resonances [14, 15] and moving loads [16]. Other mechanisms sometimes mentioned include thermo-elastic instability [17, 18], viscous instability [19] and stick-slip-separation waves [20–22].

Despite intensive research efforts, disc brake squeal propensity remains a very complex problem to predict [23], Figure 1 displays the number of publications and patents since 1935 using an internet search for 'disc brake squeal' with GOOGLE SCHOLAR. The following statistic is not complete and it can be assumed, data related to more recent years is slightly more accurate. However, for the purpose of showing trends, an internet search seems to be sufficient.

The first patent for a proposed mechanism to handle brake squeal was registered in 1936 (Period I in Figure 1) but the publication in international journals of research on this issue only started after 1969 to increase. From 1969 until 1995 (Period II), the number of annual research publications remained at a fairly low level with a total of 72 or $3.4/year$ on average. In the same period, the number of registered patents also remained quite low with a total of 32 or $1.8/year$ on average. After 1995, the number of publications began increasing, to 114 in 2009 (798 in total or $57/year$, Period III). Periods I-III are on the one hand side strongly influenced by the proprietary situation from sides of the automotive industry, but also exemplify the change of focus of customers from possessing a merely functioning automobile (period I) up to having more comfort (period III). The increase in research publications after 1999 is most likely caused by increased customers' concerns and expectations and initiated through the application of the complex eigenvalue analysis (CEA) to prediction of unstable vibration modes in the 1989 – 1990 ($\mathscr{A}$) by Liles [24]. The maximum number of patents, 14, was registered in 1999 ($\mathscr{B}$) highlighting also the practical impact of the CEA. Initially, the contact interface between pads and disc was manually tailored with springs in numerical simulations. As better contact elements were developed and implemented in commercial codes such as ABAQUS 6.4 (2003) ($\mathscr{C}$) [6], research into numerical analysis of brake squeal propensity continued to accelerate in the last decade but the number of patents actually decreased. This

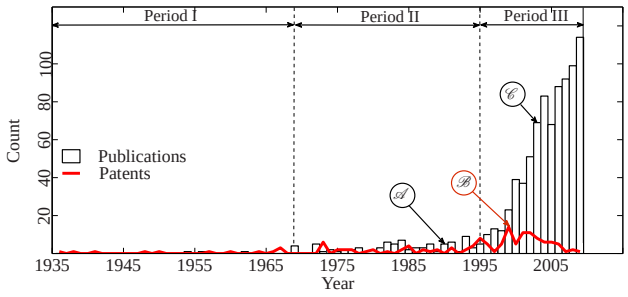

Figure 1: Literature survey 'Google Scholar': 1935-2009

could be an indication that research findings are not yet mature enough to be applied in industry. As a result, brake squeal is still of practical concern to the automotive industry as confirmed by Hoffmann and Gaul [25] or Chen [26].

Traditionally, research into brake squeal has been focused on three approaches: (a) using experimental methods to study the vibration and acoustic responses of a brake system; (b) using numerical methods, predominantly finite element models with complex eigenvalue analysis, to determine unstable vibration modes; and (c) using simplified analytical models to gain insight into the mechanism of brake squeal generation. It has been proposed by Oberst & Lai [23] that, despite the merits of these approaches, it could be beneficial to explore the use of other analysis methods for providing greater insight into the mechanism of brake squeal. For example, by applying statistical analysis to industry brake squeal test data, it has been found that the squeal performance of various pad modifications is highly correlated with the degree of non-linearity in the system [27]. Non-linear time series analysis tools and recurrence plots applied to microphone squeal test data of a full brake system illustrates the Ruelle-Takens-Newhouse route to deterministic chaos [28]. Also, in Hoffmann & Gaul [25], non-conventional analysis techniques, such as incorporating uncertainties, probabilistic measures and statistics, are recommended. Although brake squeal is essentially a deterministic problem, the exact values of many operating parameters are not known because of large variations in the material properties of notionally the same materials in identical operating conditions [29].

Empirical distributions of the friction and normal forces related to brake squeal vibrations can be found in [30, 31] where the effect of a random friction component was investigated using the discrete wavelet transform. It was found that the occurrence of squeal noise is associated with a larger mean value of the instantaneous friction coefficient and that random components of the contact forces are non-Gaussian processes. Parametric random vibrations due to friction and stochastic averaging techniques are reviewed in [32].

Incorporation of uncertainties would involve solving a governing equation with a *stochastic* component, as in [33, 34]. In order to reduce the computational resources required, instead of obtaining a deterministic solution for each variation of randomisation, a decomposition method has been developed and found to be superior to the classical Monte Carlo simulation [35]. With this decomposition method it is possible to approximate eigensolutions of a linear stochastic system.

Another way of incorporating uncertainties is to calculate the probability of squeal occurrence by means of the Monte Carlo simulation using a sub-structured and a reduced order model [36]. Randomness is taken into account through the friction coefficient, μ, the stiffness, k, or the Young‘s modulus, E, of brake components. If the input parameters of structural calculations are randomised, it is possible to couple these calculations with a parametrised CEA in ABAQUS to solve a random eigenvalue problem based on the uncertainties of key parameters such as the material properties or the friction coefficient.

The main uncertainties in disc brake squeal arise from: (1) the complexity of interacting mechanisms; (2) the still unknown functional description of the friction coefficient which is dependent on operating conditions; and (3) significant changes in the properties of the pad-lining material during operation. It has been found in a laboratory brake [37] that under varying loads, a change in pad resonances of up to 25%, due to variations in the pad-disc’s ’angle of attack’ of up to 15%, are possible. Thus a maximum change in a pad’s in-plane frequencies of $\Delta f = 11.2$kHz is possible. Due to the importance of pad vibrations, it has been suggested that a CEA should be performed, which focus on pad’s modes [37]. This has been done in [38, 39] by means of CEA, forced response calculations and the acoustic boundary element method.

Based on the study presented in [38, 39], in this paper a novel approach to predict the onset of instabilities is pursued. As linear analyses as the CEA cannot predict all instabilities [40, 41, 38], the new approach must be able to capture mechanisms different from those in the CEA which detect mode-coupling instabilities. Ideally, the procedure should be easy to understand and ready to use with commercial software packages. The new approach is complementary to the CEA and focused on certain pad modes, as suggested in [37] and studied by Oberst and Lai [38, 39]. Three key indicators are used: changes in frequency, in the kinetic energy spectrum, and the radiated acoustic power as a result of changes in the operating conditions such as the material properties of the lining materials, friction coefficient and pressure. Most research into uncertainties is focused on physical quantities such as the friction coefficient or material properties (*input* variables). This choice is somewhat arbitrary and requires time consuming calculations of a distribution of complex eigenvalues as a function of these input variables. In this study, therefore, the concept of uncertainty is quantified by *the relationship* between the changes in three output indicators: frequency, peak kinetic energy and peak acoustic power as a result of changes in the two input variables: pressure and friction coefficient. With this method, the computational efforts are significantly reduced as a statistical distribution is applied only to deterministic results (*output* variables). Further, the chosen output variables mark readily important physical design variables.

NUMERICAL MODELS

In this study, three different models are used. *Plate*-models consist of a slider on a moving plate, similar to the analytical models used in [4, 28] but with elasticity and area contact. These models represent a simplified annular disc as used in [42–45] cut open and stretched to a plate. As previous simplified brake system are fcoussed on mode-coupling instability due to the merging of the split modes [42–45], this type of instability is not expected for a plate model due to the loss of its annular structure. Although plate model II from [38] is not analysed in further detail, the numbering of the models remains the same as in [38, 39]. Further, *disc*-models consist of a pad on a moving disc.

- *Plate*-models:
  - (I) *isotropic pad*: translational moving steel plate, frequency range investigated ($0-6.5$kHz); variation: friction coefficient, pressure
  - (II) *transversely isotropic pad*: NA (studied in [38], but left out in the present paper)
- *Disc*-models:
  - (III) *isotropic pad*: rotating thick annular disc; frequency range investigated ($0.7-7.0$kHz); variation: friction coefficients; material
  - (IV) *transversely isotropic pad*: isotropic steel back - plate; rotating thick annular disc;frequency range investigated ($1-7$kHz); variation: friction coefficient, material constants with pressure

The form factor (size, geometrical features) remains the same for the isotropic/ anisotropic pad-on-disc models except that, for the anisotropic lining material, a back-plate is attached which results in higher out-of-plane stiffness. Since the total thickness remains the same, the puck‘s thickness has to be reduced by the thickness of the backplate.

The emphasis in this study is on models I and IV. Model I is used to simulate an experiment performed by Chen [26] and

model IV is used to study the influence of changes in the lining material properties (due to changes in the model's compressibility under different loads according to [46]) on Young's/shear moduli and Poisson's ratios. For both pad-on-disc systems, compliant boundary conditions, as described in [47] are taken. In Figure 2, the pad-on-plate (I) and pad-on-disc (IV) models are depicted. The material properties and mesh details are taken from [38, 39, 47].

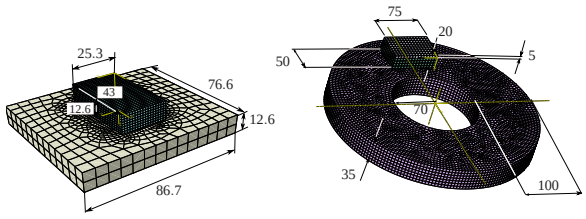

(a) isotropic pad-on-plate (b) an-istotropic pad-on-disc

Figure 2: (color online) (a) *isotropic* pad-on-*plate* model (I); (b) *anisotropic* pad-on-*disc* model (IV)

Modes of the pad-on-plate model are referred to as q_1 to q_7 according to [38] and resonances are identified in frequencies as f_1 to f_4. Apart from the resonance f_1 each of the resonances $f_2 - f_4$ house two modes, which lie very close in frequency. Due to structural and frictional damping, their peaks are merged. For the pad-on-disc systems, modes are described by (m,n,l,q), according to [48]. Here, m, n, l and q stand for out-of-plane modes with m nodal circles and n nodal lines, and in-plane radial and tangential (shear) modes, respectively. Resonances in the kinetic energy spectrum / acoustic power spectrum are identified by f_1 to f_{24} (model III) and f_1 to f_{18} (model IV) respectively, according to plots of kinetic energy & acoustic power [38, 39]. System modes, which are dominated by *pad-modes* are assigned P_x, P_y for the plate model and P_r, P_t and P_{rot} for the disc model, according to [38]. In this study, the friction coefficient μ ranges from 0.05 to 0.65 and the pressure p covers the range from 0.001 to 8.0MPa.

MODELLING OF UNCERTAINTY

The first part of this section provides insights into the problem's scope, the second introduces the probabilistic model.

Problem Scope

In modelling a brake system in order to analyse brake squeal propensity, two major unknowns are the composition and the dynamic behaviour of the brake lining as well as the exact relationship of the two mating bodies in contact expressed in terms of the friction coefficient.

When a car is slowed down in the course of the braking process, due to increased brake-line pressure, the vehicle's velocity decreases and the friction coefficient increases. With compression of the lining material, the elastic constants change non-linearly, resulting in varying material stiffness parameters [29, 46].

In Figure 3 the brake system (response) is depicted with its input (excitation) and output (squeal). In the control box, the stationary parts (caliper assembly) and the rotating brake disc are depicted. The friction coefficient and its dependency on variables is also depicted, and assigned as part of the input of the control system, inherently responsible for the feed-back loop. In many brake squeal studies it is assumed that the relative velocity between the pad and the disc, and pressurisation of the pad and its associated contact are the most important factors for mechanisms which generate squeal. Wear and temperature are little investigated compared with the aforementioned variables relative velocity and pressure, and almost nothing can be found on the dependency on humidity. That temperature has a major effect on elastic constants and therefore on frequency variations is intuitive and is briefly studied in [38], but will not be followed up in this study.

In practical engineering concerned with friction and contact, the hypothesis of COULOMB-AMONTON is of particular interest [8, 49]. However, it only accounts for a normal force with point contact and is, apart from the direction, not dependent on the absolute value of velocity [50].

In the following, the assumptions underlying this study are along the lines of findings taken from a wider study in the course of design of experiments [51]: A full brake system is tested on an industrial computer-controlled brake dynamometer as described in [51, 27]. The test consists of a total of 1669 stops and is divided into a warm and a cold section. The warm section is set up according to SAE J2521 [52] and the cold section satisfies NVH needs and customer specifications. The test conditions themselves as in SAE J2521, are designed so stringent that a problem brake system, rather squeals on the test bank than during on-vehicle tests under real operating conditions [29]. Of course, statistical data based on and derived from experiments is highly dependent on the test procedure itself. Because of the overestimative character of dynamometer tests and its derived statistics, dynamometer tests are the only true standardised benchmark of practical relevance so that, to the authors' opinion, computer simulations, in order to be of direct practical use, have to be, in the end, related to real test procedures and their statistics. Figure 4 exemplifies recorded

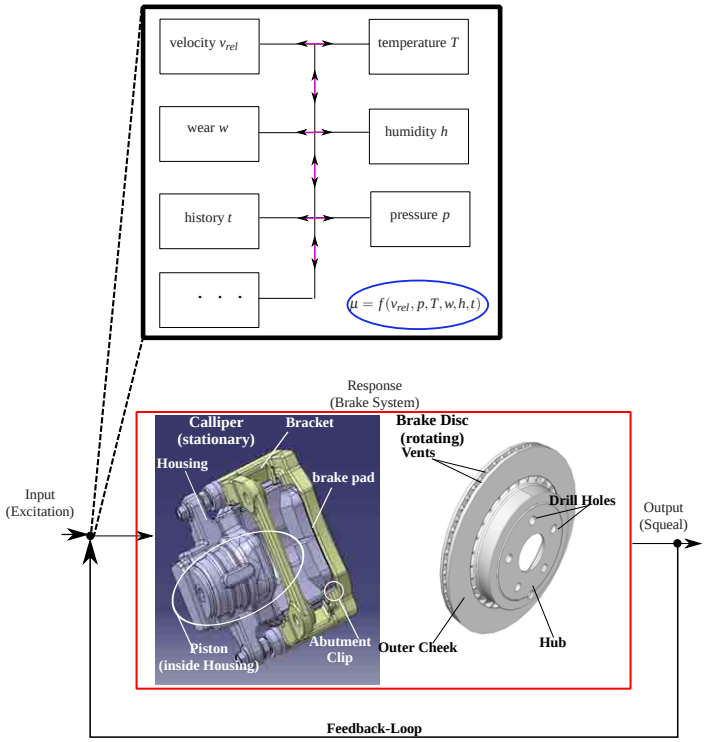

Figure 3: (color online) Schematic functional dependency of the friction coefficient and its influence on the input (excitation) of the brake system (response) prior to/during squeal.

pressure, velocity and friction coefficient data for only one stop [51]. The dashed boxes in Figure 4 (a)-(c) mark the time interval investigated in this paper (0.4 to 5.9s) for a cold forward stop of a two-piston floating calliper brake system for a mid-size sedan. The pressure in Figure 4 (a) increases linearly with 1MPa/s, as indicated by a triangle (point-slope form) at the beginning of the dashed line. The velocity in subfigure (b) de-

creases only slightly and is almost constant. In (c), the friction coefficient oscillates but tends to increase slightly. In subfigure (d), the histogram and the theoretical normal distribution of the friction coefficient data of the dashed box (Figure 4 (c)) are plotted.

The data of the friction coefficient over time is tested for normal distribution by means of a Lilliefors test with $\alpha = 0.05$ and $\alpha = 0.01$ significance levels. The null hypothesis, that the distribution comes from the family of normal distributions can only be rejected for $\alpha = 0.01$. By taking the exponential of this data, this hypothesis can no longer be rejected, hence it can be assumed that the friction coefficient data is truly log-normally distributed. From Figure 4 (d) it can be seen that the experimental data of the friction coefficient is slightly negatively skewed which results from the negative gradient of the friction coefficient curve (see also [28]). However, as in a first approach only the methodology of how to incorporate uncertainty is of interest, the assumption of normally distributed data is used for all three models at hand. The normal distribution has some advantages as it is symmetrical around its mean, and thus halves the area of the probability density function; this simplifies modelling, the calculation effort and the presentation of results. Further, in the course of the study it is assumed that the friction coefficient fluctuates very strongly due to a (i) dominant normal distributed component, with an underlying (ii) deterministic trend towards higher values due to a (iii) decreasing but almost stationary sliding velocity. All this is driven by a (iv) linearly increasing pressure. Based on these assumptions, in this paper a concept is developed related to findings of pad-mode instabilities presented in [47, 38, 39]. These pad modes

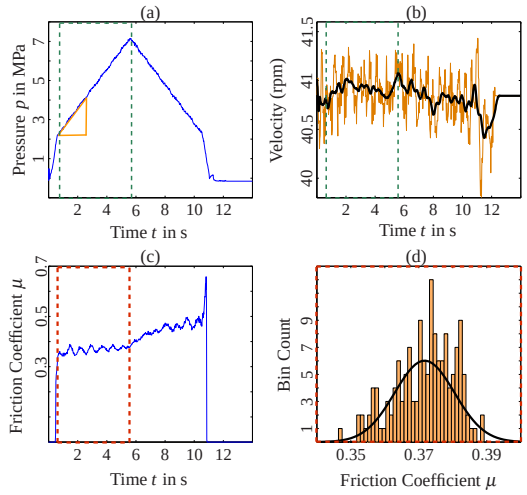

Figure 4: (colour online) Example data from experiments: (a) brake line pressure; (b) rotor velocity; (c) friction coefficient; and (d) histogram and normal distribution of part of friction coefficient curve. Data provided courtesy of PBR Ltd.

show large but variable changes in kinetic energy and seem to change their frequencies easily. The simulations performed in [47, 38, 39] depend on two varying parameters, the friction coefficient μ and the pressure p. For the anisotropic pad-on-disc model (IV), non-linear changes in the elastic constants due to different pressures are applied. In Figure 5, the development of the kinetic energy, E_k, of the isotropic pad-on-plate model (I) (Figure 2(a)) is depicted. Four resonances are marked as f_1 to f_4. For $p_0 = 1$kPa, a friction coefficient of $\mu = 0.001$, which exemplifies the friction-induced nature of the mechanisms investigated, is also applied: no peaks can be observed at $f_2 - f_4$ but as soon as μ exceeds 0.01 little peaks show up.

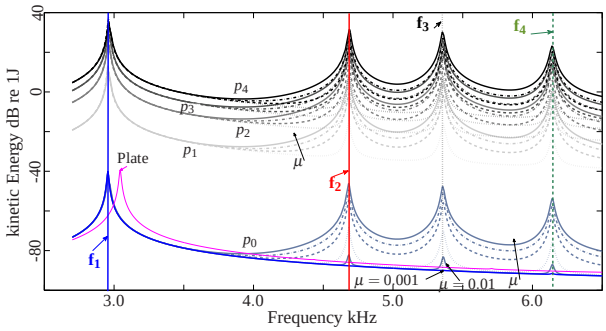

Figure 5: (color online) Kinetic energy for various pressures ($p = 1.0$kPa-8.0MPa) and friction coefficients. f_1-f_4 indicate peaks in energy spectrum

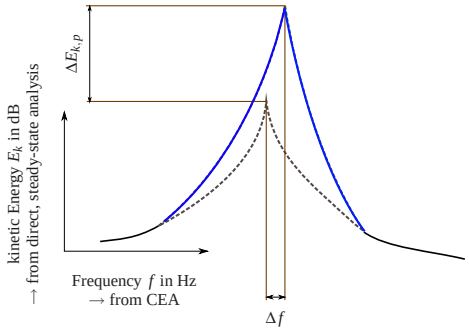

Figure 6: Sketch of problem

The problem of changes in frequency, peak kinetic energy / acoustic power is sketched and exemplified for the kinetic energy in Figure 6. Due to the braking process some of the resonance frequencies in the spectrum and their kinetic energy levels change. Most of these variable peaks are associated with in-plane pad modes which are very active in terms of vibration due to energy fed into the system and being released at their resonance frequencies is efficiently transformed in vibrations [38]. A prediction of how these pad modes behave for varying operating conditions is desirable from a design and, hence, an optimisation point of view as in for instance mixed, constrained, multi-objective problems [53]. In general, resonances are due to dominant modes which can be extracted in a CEA and are, as such, accessible for analysis in terms of mode-coupling theory and their positions in frequency. In the kinetic energy spectrum, if additional damping is applied or the pressure is high enough, not all modes might be visible anymore. This is the case for doublets of out-of-plane modes and holds also true at certain pressures for the radial and rotational pad modes P_r and P_{rot}. However, it can be hypothised that P_r and P_{rot}, due to their large changes in frequencies, adopt the function of acting as an additional perturbation in the time domain in the sense of an additional energy source superimposing changing harmonics in the time signal [38]. Therefore, it is important to know, at which frequency those, in the kinetic energy spectrum in terms of resonance peaks eliminated modes vibrate and which should not be totally neglected. For this purpose, and also to check for mode coupling instabilities, the CEA is practical. The kinetic energy, as suggested in [38], is extracted by a forced response by means of a direct, steady-state solution step and takes the role of describing the change in vibration energy by being directly related to the underlying velocity field. A change in vibration energy is important as it can be related to the external work [38], hence to feed-in energy of the system and, hence, to its self-exciting character [54]. The change in kinetic energy is the highest at those frequencies, at which the external work becomes negative. This negative external work describes work done by springs due to contact, which is not transferred into in-

ternal work and released in vibrational energy [55, 47]. Finally, changes in the acoustic power level describe the sensitivity of the system in terms of its radiated sound power, hence are directly related to brake squeal propensity.

Figure 7 exemplifies for the isotropic pad-on-plate model (I) [38] the dependency of the peak kinetic energy on (a) pressure variations with constant μ and (b) μ variations with constant pressure. According to resonances f_1 and f_3, two families of curves are formed. Each of its curves is developed by moving along the vertical lines in Figure 5 and noting down the values of peak kinetic energy for each friction coefficient at each pressure value. Clearly, the pressure dependency of the frequencies of interest can be well approximated by a quadratic function ($*$ in Figure 7) in contrast to the identical function ($**$ in Figure 7). By varying the pressure (Figure 7 (a)), the families of curves

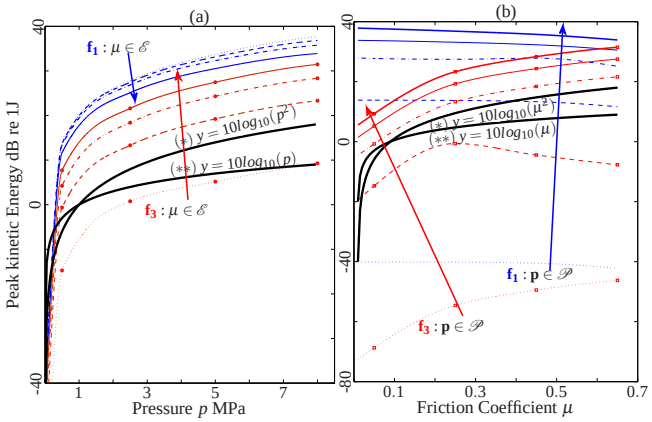

Figure 7: Scattering of peak amplitudes of kinetic energy exemplified in f_1 and f_3 by varying (a) pressure or (b) friction coefficient, by leaving either μ or p constant, respectively

look similar each, which is not the case for variations in μ (Figure 7(b)). Further, the trend of behaviour for a family of curves is very different in Figure 7 (b) from that depicted in (a). As all calculations are performed in the frequency domain, their dependency in the time domain is a-posteriori synthesised. This is done by taking the previously described time dependency of the pressure by means of an identical function and replacing pressure with time (hence identical). In that sense, the $x-$axis in Figure 7 is replaced by a surrogate, coined here as *quasi-time* $\overline{\tau}$: By doing so, modal quantities as peak kinetic energy are related to the time estimate $\overline{\tau}$. Hereby, it is further assumed that the contribution of other modes in resonance is supposedly neglegible. Based on the fact that the determination of the friction coefficient is a very difficult task, due to strong non-linear dependencies with a variation of variables (see Figure 3), in this synthesis, μ is assumed to be a random variable which has 99.9% of its probability mass within the limits of $\mu = 0.05$ and $\mu = 0.65$. With a set of calculations, for p ranging from 1kPa to 8MPa, performed in the frequency domain, their time dependence is developed by assuming μ to be Gaussian, similar to a particle in a turbulent velocity field at high Reynolds numbers [56]. In this paper, for each fixed p, the deterministic equations are solved for all μ and the complex eigenvalues, as well as the kinetic energy levels, are obtained by means of structural finite element calculations (ABAQUS 6.8-4). Then, the acoustic power level is calculated by means of the acoustic boundary element method, using a solver based on the fast multi-pole method (FMM) implemented in ESI/VAOne. For this purpose, an ABAQUS plug-in was developed in Python, which is linked to VAOne via MatLab and allows for automated calculations of probabilities.

Probabilistic Background

For the sake of simplicity, it is assumed that the distribution ($\mathscr{D}$) of the friction coefficient μ is *normal* based on the normal distribution presented in Figure 4 (d).

$$\mu \sim \mathscr{D} = \mathscr{N}(\nu, \sigma) \tag{1}$$

The change in frequency, Δf (based on eigenfrequencies of complex modes), peak kinetic energy, $\Delta E_{k,p}$, and peak acoustic power, $\Delta\Pi_p$, (both based on resonance peaks) are calculated by deterministic equations dependent on the friction coefficient μ, the pressure p and the relative velocity v_{rel}. Here, only p and μ are varied as it is assumed that the velocity is almost constant since it can decreases only very slightly in reality when it comes to a squealing event (see Figure 4 (b)). Further, it is assumed that functions of Δf, $\Delta E_{k,p}$ and $\Delta\Pi_p$ are smooth functions.

During the further course of this study, it is important that the pressure is a function of time. Then, the experimental data in Figure 4 allows for the construction of a family of functions of the form $y(x) = ax + b$. If we assume the pressure to be zero at the beginning of the test (Figure 4 (a)), which can be assumed without violation of generality, the pressure becomes an identical function ($id(x) = x$),

$$p(\overline{\tau}) = \alpha \times id(\overline{\tau}) = \overline{\tau}. \tag{2}$$

as, $\alpha = 1\text{MPa/s}$ describes the slope of a linear function.

The distribution of μ as the parameter with more uncertain dependency (Figure 7), are mapped a-posteriori onto the three variables Δf, $\Delta E_{k,p}$ and $\Delta\Pi$, in turn become normally distributed as well. The two simulation parameters p and μ are assumed to be independent from each other. In contrast to that, the frequency, the kinetic energy and the acoustic power are related and their probabilities might become conditional [57, 58]. However, their conditionality is neglected here, as a change in frequency does not necessarily mean that the kinetic energy increases and that if the kinetic energy increases strongly, for instance at mode f_4, still no significant acoustic power can be calculated at this resonance [39]. Hence, the dependency of the f, E_k and Π changes with the modes, which changes themselves due to friction and pressure. Therefore, it is here assumed that a strong dependency exists between μ and p (input variables) on the one side, Δf, $\Delta E_{k,p}$ and $\Delta\Pi_p$ (output variables) on the other side. From that it follows that the dependency between the two/three input/output values is assumed to be weak and it may be allowed to treat them as independent.

Based on that, the three random variables investigated, $V_i, i \in \{1,2,3\}$, are defined in the following by

$$V_1 = \Delta f = F(f, p(\overline{\tau})) \sim \mathscr{D}_1 \tag{3}$$
$$V_2 = \Delta E_{k,p} = F(E_k, p(\overline{\tau})) \sim \mathscr{D}_2 \tag{4}$$
$$V_3 = \Delta\Pi_p = F(\Pi, p(\overline{\tau})) \sim \mathscr{D}_3. \tag{5}$$

Here, F is a function dependent on the time dependent pressure $p(\overline{\tau})$ and either, f as the complex modes' imaginary part divided by 2π or E_k as the kinetic energy level or Π as the acoustic power level. By replacing $p(\overline{\tau})$ by $\overline{\tau}$, it is possible to see the development of Δf, $\Delta E_{k,p}$ and $\Delta\Pi_p$ as quasi-stochastic processes. Quasi due to the quasi-time dependency; stochastic, as the change in frequency, peak kinetic energy and peak acoustic power are themselves Gaussian at each time $\overline{\tau}$ (Equation (2)); and processes, as input states variable determine the output states over time [59]. For the three models at hand, it is assumed that all processes belong to the class of MARKOV

processes, as the present state is independent from a possibly underlying time history [60]. A stochastic process is exemplified by means of the change in peak kinetic energy and denoted in the following equation:

$$\{V_{2\bar{\tau}}\}_T = \{\{\Delta E_{k,p}\}_{\bar{\tau}}\}_T, \text{ with } T = [0.001, 8.0] \subset \mathbb{R}^+. \quad (6)$$

Here, $V_{2\bar{\tau}} = \Delta E_{k,p\bar{\tau}}$ marks a distribution at time $\bar{\tau}$ and $\{\}$ gives a vector of distributions [61]. T is the index set defined by a subset of $\mathbb{R}^+$ (positive real numbers, without zero) and gives the interval of time in s. As the random variables, Δf, $\Delta E_{k,p}$ and $\Delta\Pi_p$ as well as the index set T are continuous, this process is classified as *state-* and *time-continuous* [62]. As the process is random, it can be seen as the counterpart of a deterministic process [63] which is for instance described by the time trace of particle, calculated by means of classical laws of mechanic. However, for the stochastic process at each point of time, a (normal) distribution determines the probability of a change in f, $E_{k,p}$ or Π_p for each mode/ in each resonance. For the $E_{k,p}$ and Π_p, sometimes two modes are assigned to one resonance peak due to their closeness in frequency and damping effects. In practice, all numerical values are sorted into matrices of pressure over friction coefficient, according to their assigned resonance f_i. This means one gets 18 matrices in the case of model IV which are formed for all three parameters Δf, $\Delta E_{k,p}$ and $\Delta\Pi_p$, giving in the end 54 matrices with stored data. In the case of vanishing resonance peaks, as it is the case at some pressures for the radial and rotational pad modes, the modes' matrices of changes in peak energy/power are filled with zeros so that the standard deviation at these resonances has a width of zero with a mean of zero. Plotting the normal distributions for each mode or resonance, at all times and in one graph, and connecting the mean values as well as $+\sigma$ and $-\sigma$ gives the trajectory of the process [64]. Based on the data calculated, the process is taken to be a WIENER process [65] which is exemplified again for changes in peak kinetic energy and defined as follows.

$$\{V_{2\bar{\tau}}\}_T = \delta\bar{\tau} + \sigma B(\bar{\tau}) \quad (7)$$

With $\delta\bar{\tau}$ marking a drift, σ^2 the variance and $B(\bar{\tau}), \bar{\tau} \in T$ a standardised Brownian motion. The drift is responsible for the trend of the mean value, the variance describes the increase or decrease in width of two subsequent distributions. For the standardised Brownian motion, the following definition must hold true:

(1) the initial value is $B(0) = 0$ which can be assumed without losing generality for the zero pressure, $\forall V_i, i \in \{1,2,3\}$ as, with no pressure, the brake system does not squeal as no system modes are established and the differences in kinetic energy are zero.

(2 increments h of the standardised Brownian motion are normally distributed with $B(\bar{\tau}+h) - B(\bar{\tau}) \sim \mathcal{N}(0,h)$ which is one of the methodological concepts applied here. The change in μ is absorbed by the drift parameter $\delta\bar{\tau}$.

(3) the increases h_i are stochastically independent which means, for $q_i = \bar{\tau}_i + h_i$ and $s_i = \bar{\tau}_i$ with $i \in 1,2$, that $0 \le s_1 = \bar{\tau}_1 \le q_1 = \bar{\tau}_1 + h_1 \le s_2 = \bar{\tau}_2 \le q_2 = \bar{\tau}_2 + h_2$ which is true for the condition that $h_i \ge 0$ for the forward marching time. For calculations of the brake system, this means that it does not matter for the increase in peak kinetic energy if the pressure difference is low or high.

By means of a WIENER process with drift, it is possible to calculate at each time the probability of changes in frequency, peak kinetic energy or peak acoustic power according to some specified values marked by a previously defined event A. This event could be in the case of changes in peak kinetic energy, *A: the peak kinetic energy deviates by* 1dB *from its mean value*. Again, exemplified by means of changes in peak kinetic energy, it is possible to calculate the probability at each time point.

$$\{\mathscr{P}\{\Delta E_k(A)_{\bar{\tau}}\}\}_T \quad (8)$$

Here, $\mathscr{P}$ is a probability measure, which is used, to calculate the probability of $V_{2\bar{\tau}} = \Delta E_k(A)_{\bar{\tau}}, \forall\bar{\tau} \in T$. A probability is calculated at each $\bar{\tau}$ and contour plots of probability over time are obtained.

APPLICATION TO SIMPLIFIED BRAKE SYSTEMS

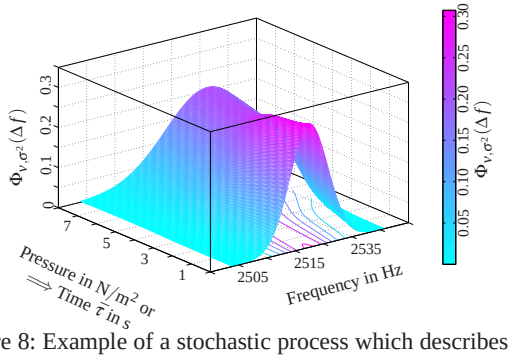

Figure 8: Example of a stochastic process which describes the variation of frequency for a $n = 3$-mode with positive travelling wave

In Figure 8 a stochastic process for the variation in frequency Δf over pressure/time of the $n = 3$ mode is depicted. $\Phi_{v,\sigma^2}(\Delta f)$ gives the value of the normal distribution of Δf dependent on the two characteristic parameters $v_{\bar{\tau}}$ and $\sigma_{\bar{\tau}}$ which change with forward marching time. For the sake of illustration, in the further course of this paper only contour plots of Δf / $\Delta E_{k,p}$ / Π_p over time of such distributions depicted in Figure 8 are used.

Isotropic Pad-on-plate

The variability in frequency and peak kinetic energy/acoustic power of all pad-on-plate (I) modes/resonances is depicted in Figure 9(a)-(c). In Figure 9(a), the pad modes P_x and P_y have the highest dispersions of frequency with increasing pressure values (Figure 9(a)). The lowest dispersions of frequency for each pressure value are given for q_1 and q_5. The trace of the process, as indicated by the mean value, might change which is especially obvious for modes q_1, q_3 and q_7 with a trend to lower frequencies with increasing pressure, rendering the process as non-stationary. The modes q_2, q_3 and q_4 are strongly influenced by the pad and the friction in the contact patch. However, a change in frequency itself does of course not say anything about the squeal propensity at resonances depicted in Figure 5, and the measure developed merely describes a mode's variability on the frequency axis (Figure 6). The higher the dispersion in frequency, the more problematic would be subsequently and traditionally applied design optimisation steps. In terms of robustness in frequency, q_3, q_4 and q_7 have to be seen as the three most problematic modes.

In Figure 9(b), the processes of changes in peak kinetic energy ($\Delta E_{k,p}$) are depicted for the isotropic pad-on-disc model (I). The wider this corridor, the more kinetic energy is likely to be released at this particular frequency. The curves do not look very spectacular, not many differences between changes in peak kinetic energy can be observed as changes in resonances f_2 to f_4 are almost congruent. However, it is visible that, for f_1, the trace of the process is negative and that the change in peak kinetic energy decreases with increasing pressure, the dispersion becomes larger which, taken together, can be interpreted as stabilising. However, for the other three frequencies, this trend cannot be observed: changes in peak kinetic energy

are positive and dispersions due to variations in the friction coefficients are expected to be high. From these results, it can be concluded that, from a design point of view, less attention should be paid to the resonance peak f_1; rather, f_2, f_3 and f_4, which give almost identical corridors, are important. Also, the development of potential changes in peak kinetic energy can be assumed to be rather constant as the variability does not greatly change its span. As the traces of f_2 to f_4, which are described by the curves formed from the mean values, are almost constant, their processes can be described as stationary with only a slightly negative drift parameter δ.

In Figure 9(c), the changes in peak acoustic power as taken from [39] are depicted. Evident is the close relationship between the traces depicted in this graph to those of peak kinetic energy depicted in Figure 9(b). Again, peaks at three frequencies, f_2 to f_4, show mostly the same behaviour which can be coined as quasi-constant. Also, based on this graph, it can be said that a system's treatment, in terms of noise measures concerning frequency f_1, requires that measures be applied that are not countermeasures against primarily friction-induced effects. If the noise is squeal, it has to be checked whether mode coupling could be the reason. As the system is also not predicted to be unstable by means of CEA, the peak at f_1 can be excluded as a possible noise source.

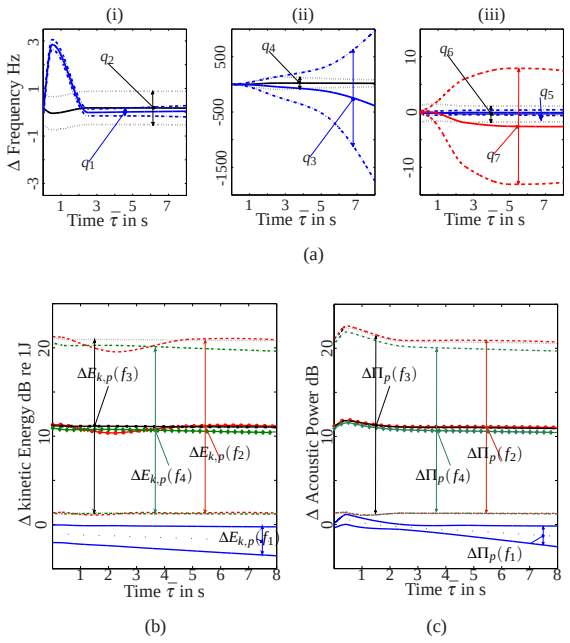

Figure 9: Stochastic processes for modes q_i of pad-on-plate system for (a) change in frequency, (b) change in peak kinetic energy and (c) change in acoustic power, respectively.

Isotropic Pad-on-disc

In Figure 10, the corridors of (a) frequency and (b) peak kinetic energy variation for the isotropic pad-on-disc model (III), under increasing pressure and varying friction coefficient, are depicted. For the sake of brevity, the processes of the acoustic power are not depicted due to their similarity to the kinetic energy. Further, only corridors of some prominent modes are exemplified: the unstable mode pairs of the $(0,3\pm,0,0)$ and $(0,5\pm,0,0)$ mode, the rotational pad mode, P_{rot}, the radial pad mode, P_r, and the tangential pad mode, P_t. The same modes were investigated in [38, 39] from the aspect of structural vibrations and acoustics. The unstable mode does not show the same mean frequency as depicted by the trace of the stochastic process in Figure 10 (ai). This is due to two effects, (1) the averaging process and (2) an imperfect merging due to frictional damping at high pressures [38]. Clearly, the corridors for the $n = 3$ modes, which are predicted to be unstable by means of the CEA, are very small which implies very little variation and uncertainty concerning possible frequency fluctuations. In contrast to that, the variations in frequency of the rotational pad mode, P_{rot}, and P_r are very strong, especially at higher pressures. This is consistent with the pad-on-plate model, where the modes with a component perpendicular to the sliding direction have very large variations in frequency. The tangential pad mode P_t only shows a much smaller variability in the low-pressure regimes than for higher pressures. Further, the rotational mode P_{rot} also shows strong deviations in frequency. In Figure 10(b), processes which describe the variability of

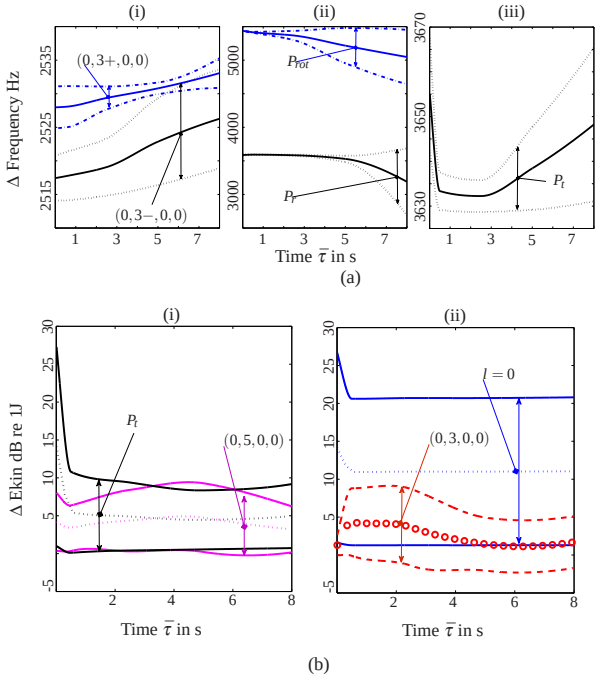

Figure 10: Corridor of variability for most prominent system modes for isotropic pad-on-disc model (III)

peak kinetic energy over time are depicted. Here, in comparison with Figure 9(b), most of the stochastic processes depicted can now be described as non-stationary. The modes with higher changes of peak kinetic energy are P_t and the in-plane tangential shear mode $l = 0$, as can be seen using the scale of the y-axis. The $l = 0$ mode, does not vary in frequency at all, therefore, its stochastic process of Δf is not depicted here. From the out-of-plane disc modes-dominated system modes, only the unstable $n = 3$ and the stable $n = 5$ modes show wider dispersion values in changes of kinetic energy. The radial pad mode and the rotational pad mode are not depicted in terms of their changes in kinetic energy, as after $p = 0.5$MPa no resonance at their frequency is visible anymore.

Anisotropic Pad-on-disc

For the anisotropic pad-on-disc model (IV), the rotational pad mode, P_{rot}, and the radial pad mode, P_r, show significant changes in frequency, as depicted in Figure 11 (a) (i-iii). Other modes show negligible variations. In Figure (b) and (c), the variations in frequency of the only as unstable predicted mode pair, $(0,3\pm,0,0)$, and the tangential pad mode, P_t, are depicted. In comparison with the isotropic pad-on-disc model III (Figure 10 (aii)), the change in frequency of the radial and rotational pad mode in Figure 11 (a) is much stronger at lower pressures, indicating a higher sensitivity of these modes due to changed lining. The tangential pad mode P_t (c) shows a similar dip as the P_t of model III (Figure 10 (aiii)). Similar to the isotropic

pad-on-disc model, modes P_r and P_{rot} do not show significant kinetic energy peaks after $p = 0.5$MPa, and are thus not depicted here.

Calculation of Probabilities

As the stochastic processes of changes in modal frequencies, changes in peak kinetic energy and peak acoustic power have been calculated in the previous section, it is now possible to calculate the probability that these variables change by either (1) a certain percentage or (2) a certain value. Even though it might be interesting to look for the probability of a certain percentage deviation, it is of more interest to search specifically for a certain deviation in kinetic energy or frequency and, hence, the percentage changes in each mode. In the following, probability calculations for the isotropic pad-on-plate model (I) are performed as an example. In Figure 12(a), the probability density function and in Figure 12(b) its cumulative density function are depicted for mode f_1 of the kinetic energy plot for a pressure $p = 10^{-3}$MPa. Exemplified is the calculation of the probability of the event that the kinetic energy increase deviates about 25% from the mean increase in kinetic energy. For the first mode, f_1, this probability is around 40%. In the following, this procedure is repeated over time which allows the calculation of probabilities plotted to be in the form of traces.

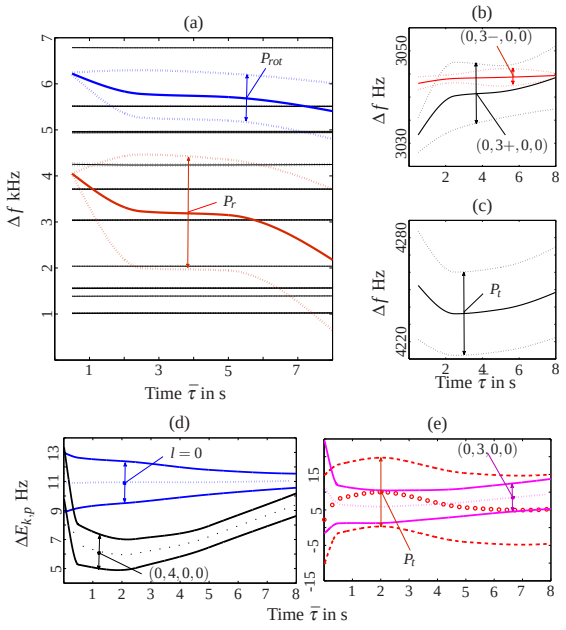

Figure 11: Corridor of variability of anisotropic pad-on-disc model (IV) for changes in frequency of (a) all system modes, (b) unstable mode pair $(0,3,\pm,0,0)$ (i), pad mode (ii)

Plots of probabilities due to changes in frequency (Figure 13) and kinetic energy (Figure 14) over pressure for the simplistic pad-on-plate model (I) are depicted. As the frequency change of q_2 is negligibly small, it is not depicted here. Each graph represents the probability that either the frequency deviation from the mean frequency (event A) or the kinetic energy deviation from the mean kinetic energy (event B) is either smaller than, or equal to, an assumed frequency or energy level (A: $\Delta f \in \{10, 20, ..., 100\text{Hz}\}$, $B : \Delta E_k \in \{1, 2, 10\}$). As can be seen in Figure 13, P_x and P_y show the highest likelihoods of changing their frequencies irrespective of the values applied. For the other modes, only small changes in frequencies, up to 30Hz, have a probability greater than 0.02%. For changes in peak kinetic energy (Figure 14), it can be observed that the resonance in f_1 (see Figure 5) shows a higher probability of changing its kinetic energy but only up to 2dB whereas the other

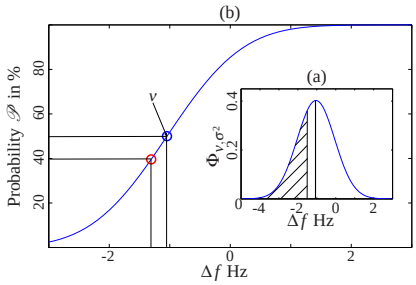

Figure 12: Example of calculating probability of cumulative density function (Probability calculated in terms of deviation of position parameter taken as trace of median of stochastic process and then normalising probabilities to cumulative density of median

three resonances show higher probabilities up to changes of 10dB. As, from those graphs, a detailed analysis and comparisons of different systems is difficult to accomplish, the averaged probabilities for pressures from 0.001 to 8.0MPa for selected frequencies, peak kinetic energies/acoustic powers are depicted in Table 1. In this table, $\mathscr{P}_1$, $\mathscr{P}_2$ and $\mathscr{P}_3$ stand for the probabilities that the frequency, peak kinetic energy and peak acoustic power, respectively, change according to previously chosen values. Here, it is stipulated that the higher the proba-

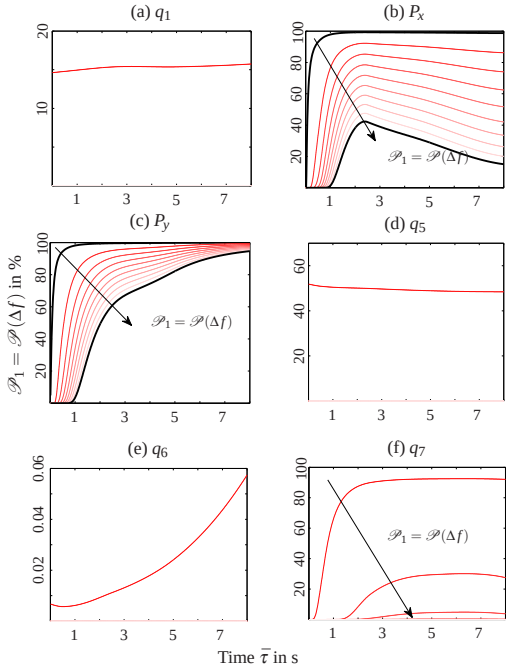

Figure 13: Probabilities for different variations of frequency of modes q_1 to q_4 for pad-on-plate system (model I)

bility, the less controllable is the brake system's behaviour at that frequency. For the energy related terms, $E_{k,p}$ and Π_p, it is assumed that only for positive growth released vibrations are high or that squeal propensity increases, respectively. This means, especially for the first three modes of the isotropic pad-on-disc system (III) that the propensity of squeal decreases. It can be readily seen in table 1 which of the modes it is important to treat in terms of squeal propensity. However, by introducing an arbitrary chosen value of change in frequency, kinetic energy or acoustic power, it becomes necessary to arrive at an overall conclusion. Therefore, similar to the plots of frequencies over real parts to show squeal propensity by means of the CEA (see Figure 3 in Ouyang et al. [6]), the averaged uncertainty for each mode is calculated. As squeal can appear at a change of either 1dB or 10dB kinetic energy or

acoustic power, the three probabilities of Table 1 are equally weighted and plotted in Figure 17 for the three simplified systems. The (averaged) probabilities of Δf, $\Delta E_{k,p}$ and Π_p allow design goals to be tackled differently. As the three parameters are assumed to be independent their probabilities were simply multiplied and normalised by the maximum of all products: $\Psi = \mathscr{P}_1\mathscr{P}_2\mathscr{P}_3/MAX$. The value of Ψ is depicted by bars and provides an overall and absolute measure of *exigency to change the design*. From Figure 17 (a), it is possible to conclude that it is necessary to assess mode 3, and then mode 3 and mode 7, with the goal of minimising Ψ of these modes. For the stability of model III, it appears that, firstly, the probabilities of modes 11 (P_r) and 12 (P_t), and the rotational pad mode 17 should be minimised. Meanwhile, the probability of neighbouring modes that is modes $7/8$ for the radial pad mode and modes $15/16$ and 18 for the rotational pad mode, should also be monitored in optimisation runs. These neighbouring modes are strongly influenced by pad modes and were found oscillating in terms of acoustic power over μ [38]. So far, only the probability

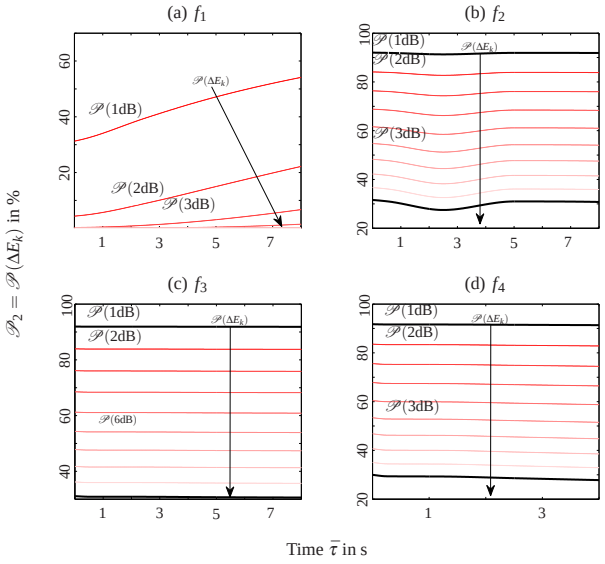

Figure 14: Probabilities for different kinetic energy of resonances f_1 to f_4 for the pad-on-plate system (model I)

over the whole pressure range averaged over three frequency, kinetic energy and acoustic power values is considered. As it is assumed in [38, 39] that pad modes, here especially the radial and rotational pad mode, lead directly to squeal only in low pressure regimes, non-averaged values for pressures from 1kPa to 1MPa are calculated next (Figure 18). Evidently, the changes in f, $E_{k,p}$ and Π_p are still significant for the pad modes whereas other modes, including those predicted by the CEA to be unstable, do not show higher values of Ψ. This exemplifies that the pad modes are likely to cause squeal in low-pressure regimes. With higher pressures, they are partially eliminated. However, at the same time, for low pressures the frequency changes of these pad modes are not as strong as for higher pressures. At higher pressures, pad modes P_r and P_t change their function: from being squeal sources, they might act as disturbing functions and change their frequencies. This might work as an additional energy source which could induce or amplify the mode-coupling mechanism. From the design point of view, it is important to keep an eye on the regime where the pad modes fluctuate in frequency and are not eliminated in the resonance spectrum at the same time.

Table 1: Probabilities of Δf change in frequency $\mathscr{P}_1 = \mathscr{P}(\Delta f)$, ΔE_k in peak kinetic energy $\mathscr{P}_2 = \mathscr{P}(\Delta E_{k,p})$ and $\Delta\Pi$ in peak acoustic power $\mathscr{P}_3 = \mathscr{P}(\Delta\Pi_p)$ in %

Mode	Resonance	CEA	(I) $\mathscr{P}_1$ (1,50,100)Hz	$\mathscr{P}_2$ (1,5,10)dB	$\mathscr{P}_3$ (1,5,10)dB
1	f_1		(15,0,0)	(0,1,0)	(4,0,0)
2	f_2		(0,0,0)	(92,60,30)	(96,81,64)
3	f_2		(94,54,24)	(92,60,30)	(96,81,64)
4	f_3		(98,77,47)	(92,61,31)	(96,81,63)
5	f_3		(23,0,0)	(92,61,31)	(96,81,63)
6	f_4		(0,0,0)	(92,60,29)	(96,81,62)
7	f_4		(75,0,0)	(92,60,29)	(96,81,62)
Mode	Resonance	CEA	(III) $\mathscr{P}_1$ (10,30,70)Hz	$\mathscr{P}_2$ (1,3,7)dB	$\mathscr{P}_3$ (1,3,7)dB
1	f_1		(7,0,0)	(0,0,0)	(29,0,0)
2	f_1		(0,0,0)	(0,0,0)	(29,0,0)
3	f_2		(1,0,0)	(23,0,0)	(21,0,0)
4	f_3		(0,0,0)	(24,0,0)	(22,0,0)
5	f_3		(0,0,0)	(24,0,0)	(22,0,0)
6	f_4		(0,0,0)	(96,89,74)	(0,0,0)
7	f_5	✔	(8,0,0)	(87,62,27)	(86,59,24)
8	f_5	✔	(0,0,0)	(87,62,27)	(86,59,24)
9	f_6		(0,0,0)	(87,62,27)	(93,80,55)
10	f_6		(0,0,0)	(92,77,50)	(93,80,55)
11	P_r		(57,37,27)	(45,39,33)	(45,40,33)
12	P_t		(21,2,1)	(91,75,45)	(93,79,54)
13	f_9		(11,0,0)	(60,13,0)	(50,8,0)
14	f_9		(0,0,0)	(60,13,0)	(50,8,0)
15	f_{10}		(5,0,0)	(96,88,72)	(96,87,70)
16	f_{10}		(0,0,0)	(96,88,72)	(96,87,70)
17	P_{rot}		(84,70,53)	(37,29,25)	(35,27,24)
18	f_{12}		(0,0,0)	(1,0,0)	(0,0,0)
19	f_{13}	✔	(0,0,0)	(90,71,39)	(90,71,39)
20	f_{13}	✔	(2,0,0)	(90,71,39)	(90,71,39)
21	f_{14}		(0,0,0)	(0,0,0)	(0,0,0)
22	f_{14}		(0,0,0)	(0,0,0)	(0,0,0)
23	f_{15}		(3,0,0)	(89,69,35)	(89,68,34)
24	f_{15}		(0,0,0)	(89,69,35)	(89,68,34)
Mode	Resonance	CEA	(IV) $\mathscr{P}_1$ (10,50,70)Hz	$\mathscr{P}_2$ (1,5,7)dB	$\mathscr{P}_3$ (1,5,7)dB
1	f_1		(7,0,0)	(27,0,0),	(28,0,0)
2	f_1		(0,0,0)	(27,0,0)	(28,0,0)
3	f_2		(1,0,0)	(8,0,0)	(13,0,0)
4	f_3		(6,0,0)	(4,0,0)	(7,0,0)
5	f_3		(0,0,0)	(4,0,0)	(7,0,0)
6	f_4		(0,0,0)	(93,66,54)	(0,0,0)
7	f_5	✔	(9,0,0)	(94,70,60)	(93,68,57)
8	f_5	✔	(9,0,0)	(94,70,60)	(93,68,57)
9	f_6		(0,0,0)	(92,63,50)	(92,62,50)
10	f_6		(0,0,0)	(92,63,50)	(92,62,50)
11	P_r		(91,88,86)	(60,40,34)	(48,41,39)
12	P_t		(69,11,2)	(94,71,60)	(94,71,60)
13	f_9		(0,0,0)	(17,0,0)	(34,1,0)
14	f_9		(0,0,0)	(17,0,0)	(34,1,0)
15	f_{10}		(1,0,0)	(96,78,69)	(95,76,67)
16	f_{10}		(0,0,0)	(96,78,69)	(95,76,67)
17	P_{rot}		(94,84,80)	(38,27,25)	(39,27,25)
18	f_{12}		(0,0,0)	(4,0,0)	(34,8,4)

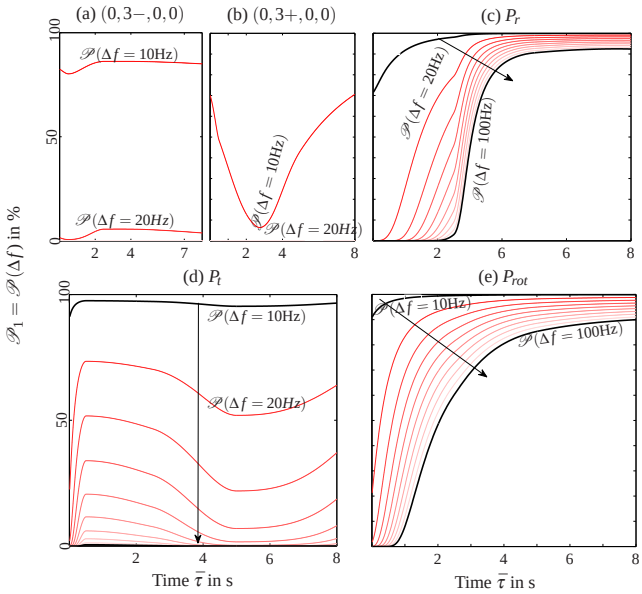

Figure 15: Probability of frequency variation 10 Hz to 100 Hz for selected modes of the isotropic pad-on-disc model (III).

CONCLUSION

In this paper, a probabilistic approach, which applies uncertainty prior to deterministic calculations of a brake system, is presented. The uncertainty lies in the exact development of (a) changes in frequency, (b) in developing vibrations represented by the kinetic energy and (c) radiated acoustic power while brake line pressure is increased and the vehicle is slowed down. From experimental data, it is found that the friction coefficient

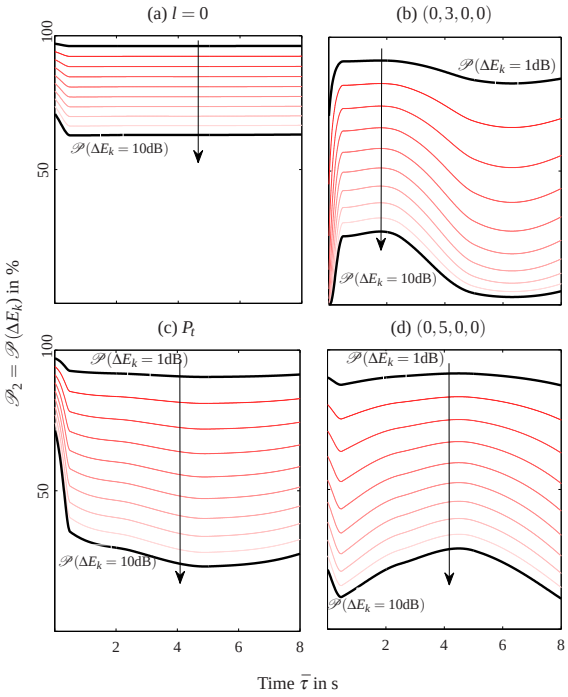

Figure 16: Probabilities for changes in kinetic energy for selected modes of isotropic pad-on-disc model (III).

is approximately normally distributed in the regime with linearly increasing pressure and represents a linear function of time. The normal distribution of the friction coefficient data is mapped on deviations in frequency derived from the CEA, and the kinetic energy is calculated by a direct, steady-state response analysis and acoustic power [38, 39]. By this procedure, a time-continuous stochastic process, namely, a Wiener process, is formed whereby it is possible to calculate, by means of probability measures, the uncertainties of the variable behaviour of a brake system due to changes in the response spectrum. This probability can be seen as an indicator of brake squeal propensity. To calculate the uncertainty measure, the following steps have to be performed.

(1.) A CEA over various pressures, p_i, and friction coefficients, μ_j, gives mean values and standard deviations of the complex modes' frequencies and indicates which mode is predicted to be unstable in terms of mode coupling. The mean values of the frequencies form a corridor with their standard deviations over pressures.

(2.) The kinetic energy spectrum, calculated by means of the direct, steady-state analysis, delivers locations of the highest fed-in energy for pressures, p_i, and friction coefficients, μ_k, for which $\mu_k = \mu_j$ is not necessarily required.

(3.) The peak kinetic energies are selected for each μ_k and p_i, and are tabulated for each mode in order to calculate their standard deviations due to pressure and increases in friction coefficients. Plotting the peak kinetic energy over p_i or μ_k gives their dependency and forms a corridor from which the mean values of the minimum and maximum boundaries are isolated.

(4.) As in (3.) but, this time, for the acoustic power after acoustic calculations by means of, for instance, the boundary element method or (even faster) the ERP method [45, 47].

(5.) Over each corridor's mean value of the formed corridors, a normal distribution can be found which produces a continuous stochastic process.

(6.) For each normal distribution, a probability can be calculated. As the possible dispersion of modes in resonance is of interest, a certain deviation from the stochastic process' position parameter is requested. This can be done for either each time point or intervals of pressure.

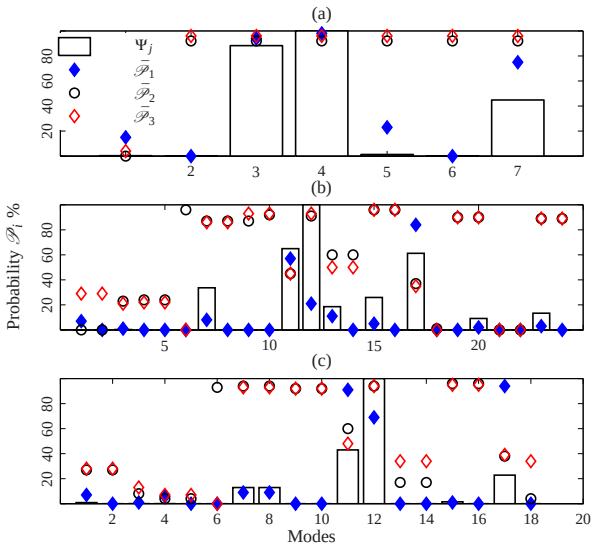

Figure 17: Probabilities of changes in frequency of 10Hz, changes in kinetic energy and acoustic power of 1dB and joint probability over pressure range of 0.001 to 8MPa

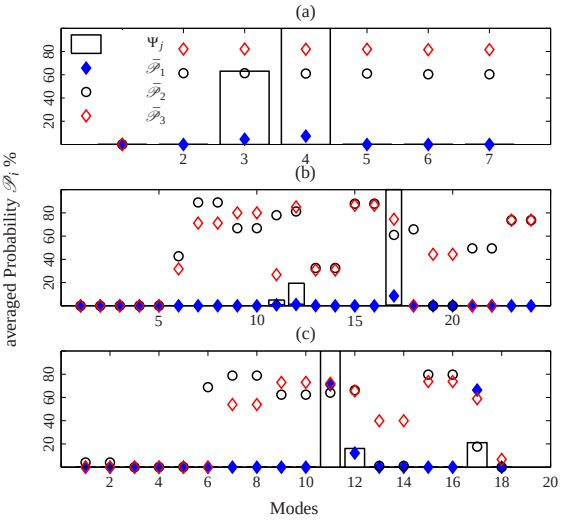

Figure 18: Models I, III and IV: Averaged probabilities $\bar{\mathscr{P}}_i$ of changes in frequency of $\Delta f \in \{10, 30, 50\}$Hz, changes in kinetic energy and acoustic power of $\Delta E_k, \Delta\Pi \in \{1, 3, 5\}$dB and joint probabilities for only low pressure regime 0.001 to 1MPa

If a different distribution, other than the mean values and standard deviations of the normal distribution, is taken, other position and dispersion parameters have to be calculated. A non-

symmetrical distribution doubles the calculation effort but does not change the methodology.

Since the degree of uncertainty is applied after deterministic calculations via the finite and the boundary element method on a limited number of frequencies, as only the peaks are of interest, the computational costs are lower than, for instance, those accrued by a Monte Carlo simulation. The method is straightforward, can be enlarged by incorporating different velocities or temperatures and is easily implemented and automated by means of a plug-in function in Python which reads out results from ABAQUS (FEM) and VAOne (BEM), respectively. Finally, a probability is obtained which, as a measure complements the CEA, but is in the end also superior to the CEA alone, in the sense that it incorporates released feed-in energy [38] as an indication of vibrational activity [54, 66]. It is exemplified that the pad modes, apart from the unstable modes(CEA), show an overall tendency to induce squeal. This instability is not predicted by the CEA but has been evidenced by calculations of kinetic energy, non-linear time series analyses [38] and calculations of radiated acoustic power [39]. Here, it is quantified by probability measures which can be used in an optimisation process in order to gain higher squeal stability. The application of stochastic processes and their calculations, in terms of squeal propensity measures, will be performed in the near future on the real geometry of a brake system to test the validity of the proposed method.

ACKNOWLEDGEMENTS

This research was undertaken on the NCI National Facility in Canberra, Australia, which is supported by the Australian Commonwealth Government. The first author acknowledges receipt of a University College Postgraduate Research Scholarship for the pursuit of this study and the Australian Acoustical Society for a *Young Scientist's Award* to participate at the ICA2010 Conference. Also, the authors would like to thank PBR Pty Ltd and, especially, Dr. Antti Papinniemi, for the provision of measurement data from an industrial noise dynamometer.

REFERENCES

[1] A. Akay. Acoustics of friction. *Journal of the Acoustical Society of America*, 111(4):1525–1548, 2002.

[2] H. Abendroth and B. Wernitz. The integrated test concept: Dyno-vehicle, performance-noise. *SAE Technical Paper Series*, 2000-01-2774, 2000.

[3] M. Yang and P.Blaschke Afaneh, A.-H. A study of disc brake high frequency squeal and disc in-plane / out-of-plane modes. *SEA Technical Papers*, 2003-01-1621:1–8, 2003.

[4] N. Hinrichs, M. Oestreich, and K. Popp. On the modelling of friction oscillators. *Journal of Sound and Vibration*, 216(3):435–459, 1998.

[5] N.M. Kinkaid, O.M. O'Reilly, and P. Papadopoulos. Automotive disc brake squeal. *Journal of Sound and Vibration*, 267:105 – 166, 2003.

[6] H. Ouyang, W. Nack, Y. Yuan, and F. Chen. Numerical analysis of automotive disc brake squeal: a review. *International Journal of Vehicle Noise and Vibration*, 1:207–231, 2005.

[7] F. P. Bowden and L. Leben. Nature of sliding and the analysis of friction. *Nature*, 3572:691–692, 1938.

[8] F. P. Bowden and D. Tabor. Mechanism of metallic friction. *Nature*, 3798:197–199, 1942.

[9] C.M. Mate, G.M. McClelland, R. Erlandsson, and S. Chiang. Atomic-scale friction of a tungsten tip on a graphite surface. *Phys. Rev. Lett.*, 59:1942–1945, 1987.

[10] H.R. Mills. Brake squeak. Technical report, The Institution of Automobile Engineers, Research Report, 9000 B and 9162 B, 1938.

[11] R.T. Spurr. A theory of brake squeal. *Proceedings of the Automobile Division, Institution of Mechanical Engineers 1961-1962 (1)*, 1:33 – 52, 1961.

[12] M.R. North. Disc brake squeal - a theoretical modell. Technical Report 5, Motor Industry Research Association, Warwickshire, England, 1972.

[13] S.K. Rhee, P.H.S. Tsang, and Y.S. Wang. Friction-induced noise and vibration of disc brakes. *Wear*, 133:39–45, 1989.

[14] J.E. Mottershead, H. Ouyang, M.P. Cartmell, and M.I. Friswell. Parametric resonances in an annular disc with a rotating system of distributed mass and elasticity: And the effects of friction and damping. *Proceedings: Mathematical, Physical and Engineering Sciences*, 453(1956):1–19, 1997.

[15] H. Ouyang, J.E. Mottershead, M.P. Cartmell, and M.I. Friswell. Friction-induced parametric resonances in discs: effect of a negative friction-velocity relationship. *Journal of Sound and Vibration*, 209(2):251–264, 1998.

[16] H. Ouyang. Moving loads and car disc brake squeal. *Noise & Vibration WORLDWIDE*, 34(11):7–15, December 2003.

[17] J.R. Barber. The influence of thermal expansion on the friction and wear process. *Wear*, 10(2):155 – 159, 1967.

[18] J.R. Barber. Thermoelastic instabilities in the sliding of conforming bodies. *Royal Society of London Proceedings Series A Mathematics Physics and Engineering Science*, 312(1510):381 – 394, 1969.

[19] N. Hoffmann and L. Gaul. Effects of damping on mode-coupling instability in friction induced oscillations. *ZAMM, Z. Angew. Math. Mech.*, 83(8):524–534, 2003.

[20] G.G. Adams. Self-excited oscillations of two elastic half-spaces sliding with a constant coefficient of friction. *ASME Journal of Applied Mechanics*, 62:867–872, 1995.

[21] G.G. Adams. Steady sliding of two elastic half-spaces with friction reduction due to interface stick-slip. *ASME Journal of Applied Mechanics*, 65:470–475, 1998.

[22] V. Linck, L. Baillet, and Y. Berthier. Modelling the consequences of local kinematics of the first body on friction and on the third body sources in wear. *Wear*, 255:299–308, 2003.

[23] S. Oberst and J. Lai. A critical review on brake squeal and its treatment in practice. In *Internoise 2008, Shanghai*, 2008.

[24] G.D. Lilis. Analysis of disc brake squeal using finite element methods. *SAE Technical Papers*, 891150:249–257, 1989.

[25] N. Hoffmann and L. Gaul. Friction induced vibrations of brakes: Research fields and activities. *SAE Technical Paper Series*, 2008-01-2579:1–8, 2008.

[26] F. Chen. Automotive disk brake squeal: an overview. *International Journal of Vehicle Design*, 51(1/2):39–72, 2009.

[27] S. Oberst, J. C. S. Lai, S. Moore, A. Papinniemi, S. Hamdi, and D. Stanef. Statistical analysis of brake squeal noise. In *Internoise 2008, Shanghai*, 2008.

[28] S. Oberst, J. C. S. Lai, S. Moore, A. Papinniemi, S. Hamdi, and D. Stanef. Chaos on brake squeal noise. In *Internoise 2008, Shanghai (China)*, 2008.

[29] F. Chen, F. Tan, C./Chen, C. A. Tan, and R. L. Quaglia. *Disc Brake Squeal: Mechanism, Analysis, Evaluation and Reduction/Prevention*. SAE-Society of Automotive Engineers, 2006.

[30] R. A. Ibrahim, S. Madhavan, S. L. Qiao, and W. K. Chang. Experimental investigation of friction-induced noise in disc brake systems. *International Journal of Vehicle Design*, 23:218–240, 2000.

[31] D.M. Beloiu and R. A. Ibrahim. Analytical and experimental investigations of disc brake noise using the frequency-time domain. *Structural Control and Health Monitoring*, 13:277–300, 2006.

[32] J.B. Roberts and P.D. Spanos. Stochastic averaging: An approximate method of solving random vibration problems. *International Journal of Non-Linear Mechanics*, 21(2):111–134, 1986.

[33] K. Sepahvand. *Uncertainty Quantification in Stochastic Forward and Inverse Vibration Problems Using Generalized Polynomial Chaos Expansions*. PhD thesis, Technische Universität Dresden, Fakultät für Maschinenwesen, Institut für Festkörpermechanik, 2008.

[34] Z.L. Huang and X.L. Jin. Response and stability of a sdof strongly nonlinear stochastic system with light damping modeled by a fractional derivative. *Journal of Sound and Vibration*, 319:1121–1135, 2009.

[35] S. Rahman. Stochastic dynamic systems with complex-valued eigensolutions. *International Journal for Computational Methods in Engineering*, 71:963Ű986, 2007.

[36] A. Culla and F. Massi. Uncertainty model for contact instability prediction. *Acoustical Society of America*, 126(3):1111–1119, 2009.

[37] O. Giannini and A. Sestrieri. Predictive model of squeal noise occuring on a laboratory brake. *Journal of Sound and Vibration*, 296:583 – 601, 2006.

[38] S Oberst and J.C.S. Lai. Numerical study of friction-induced pad mode instability in brake squeal. In *20th International Congress on Acoustics (ICA 2010) in Sydney, 23 - 27 August, Australia*, 2010.

[39] S Oberst and J.C.S. Lai. Acoustic radiation of instantaneous modes in brake squeal. In *20th International Congress on Acoustics (ICA 2010) in Sydney, 23 - 27 August, Australia*, 2010.

[40] M.T. Bengisu and A. Akay. Stability of friction-induced vibrations in multi-degree-of-freedom systems. *Journal of Sound and Vibration*, 171:557–570, 1994.

[41] N.M. Kinkaid, O.M. O'Reilly, and P. Papadopoulos. On the transient dynamics of a multi-degree-of-freedom friction oscillator: a new mechanism for disc brake noise. *Journal of Sound and Vibration*, 287:901–917, 2005.

[42] S. Oberst and J.C.S. Lai. Acoustic response of a simplified brake system by means of the boundary element method. In *NOVEM2009, Keble College, Oxford, England, 5-8April*, 2009.

[43] S. Oberst and J.C.S. Lai. Numerical analysis of a simplified brake system. In *NOVEM2009, Keble College, Oxford, England,5-8April*, 2009.

[44] S. Oberst and J.C.S. Lai. Non-linear analysis of brake squeal. In *ICSV16, Krakow, 5-9 July*, 2009.

[45] S. Oberst and J.C.S. Lai. Numerical prediction of brake squeal propensity using acoustic power calculation. In *Proceedings of ACOUSTICS 2009*, 2009.

[46] D. Yuhas, J. Ding, and S. Vekatesan. Non-linear aspects of friction material elastic constants. *SEA Technical Papers*, 2006-01-3193:1–10, 2006.

[47] S Oberst and J.C.S. Lai. Methodology of numerically simulating brake squeal noise by means of a simplified brake system. In *20th International Congress on Acoustics (ICA 2010) in Sydney, 23 - 27 August, Australia*, 2010.

[48] H. Lee and R. Singh. Acoustic radiation from out-of-plane modes of an annular disk using thin and thick plate theories. *Journal of Sound and Vibration*, 282(1-2):313–339, April 2005.

[49] J.T Oden and J.A.C. Martins. Models and computational methods for dynamic friction phenomena. *Computational Methods in Applied Mechanics and Engineering*, 52:527–634, 1985.

[50] J. Awrejcewicz and P. Olejnik. Analysis of dynamic systems with various friction laws. *Applied Mechanics Reviews*, 58:389–411, November 2005.

[51] S. Moore, J.C.S. Lai, S. Oberst, A. Papinniemi, Z. Hamdi, and D. Stanef. Design of experiments in brake squeal. In *Internoise 2008*, 2008.

[52] Surface vehicle recommended practice, disc and drum brake dynamometer squeal noise matrix. Technical report, SAE J2521, 2006.

[53] T. Ray and K. M. Liew. A swarm metaphor for multiobjective design optimisation. *Engineering Optimization*, 34(2):141–153, 2002.

[54] D. Guan and J. Huang. The method of feed-in energy on disc brake squeal. *Journal of Sound and Vibration*, 261:297–307, 1994.

[55] Dassault Systemes. *ABAQUS/CAE User's MANUAL*, 2007.

[56] D.J. Thomson. Criteria for the selection of stochastic models of particle trajectories in turbulent flows. *Journal of Fluid Mechanics*, 180:529–556, 1986.

[57] G.R. Shorack. *Probability for statisticians*. Springer: New York, 2000.

[58] S. Huschens. *Theorie und Methodik der Statistik*. Technische Unisverität Dresden, Institut für quantitative Verfahren, insbesondere Statistik, Vorlesungsskript, 7. Auflage, Oktober, 2007.

[59] R. Bellmann. On the theory of dynamic programming. *Proceedings of the National Academy of Sciences of the United States of America*, 38(8):716–719, 1952.

[60] J.C. Hull. *Options, Futures, and Other Derivatives*. Prentice Hall, 2005.

[61] P. Embrechts, C. Klüppelberg, and T. Mikosch. *Modeling Extremal Events for insurance and finance*. Berlin, New York: Springer-Verlag, 1996.

[62] A. Spanos. *Probability Theory and Statistical Inference*. Cambridge University Press, UK, 1999.

[63] K. Itô, editor. *Turing Machines*, volume 1. Cambridge, MA: MIT Press„ 2 edition, 1987.

[64] J.L. Doob. What is a stochastic process? *The American Mathematical Monthly*, 10:648–653, 1942.

[65] D.J. Thomson. On the relative dispersion of two particles in homogeneous stationary turbulence and the implication for the size of concentration fluctuations at large times. *Journal of the Royal Meteorological Society*, 112:890–894, 2006.

[66] A. Papinniemi. *Vibro-acoustic Studies of Brake Squeal Noise*. PhD thesis, School of Aerospace, Civil and Mechanical Engineering, The University of New South Wales, Australian Defence Force Academy, 2007.